Hejazi S
Cardiff University
School of Engineering

Packianather M
Cardiff University
School of Engineering

Liu Y
Cardiff University
School of Engineering

ADVANCED MANUFACTURING

Using DCGAN and WGAN-GP to Generate Artificial Thermal RGB Images for Induction Motors

The paper investigates the feasibility of using GANs to create realistic induction motor thermal RGB image datasets for multimodal condition-monitoring systems. Generating high-quality thermal images presents computational challenges, and in this study, two GAN frameworks, DCGAN and WGAN-GP, were used under different health conditions. Firstly, DCGAN was used on three conditions using various hyperparameters, but the results required further improvement. Secondly, WGAN-GP was used with an extensive training duration of 11 hours, utilising 10,000 epochs and a batch size of 64, targeting the inner fault dataset, which resulted in generating artificial images that closely resembled real images. This study highlights the impact of hyperparameters on GAN performance and demonstrates the capability of GANs in creating artificial thermal image datasets.

Keywords:
Condition monitoring, generative adversarial networks, thermal images, DCGAN, WGAN-GP.

Corresponding author:
HejaziS@cardiff.ac.uk

S. Hejazi, M. Packianather, and Y. Liu, 'Using DCGAN and WGAN-GP to Generate Artificial Thermal RGB Images for Induction Motors', *Proceedings of the Cardiff University Engineering Research Conference 2023*, Cardiff, UK, pp. 113-117.

doi.org/10.18573/conf1.aa

INTRODUCTION

In the era of Artificial Intelligence (AI) and smart manufacturing, having a reliable condition monitoring system for fault detection and recognition is essential for maintaining high-quality standards and controlling the production process [1]it is difficult to obtain a sufficient defect data set in terms of diversity and quantity. A new generation method called surface defect-generation adversarial network (SDGAN. This paper follows the paper published by Hejazi et al. published on December 2022. This study aims to highlight the importance of using a multimodal condition monitoring system utilising vibration and thermal images to increase the fault detection accuracy [2]. Thermal images are considered promising in induction motor condition monitor it can reach up to 100% if images are clear without further preprocessing [3], unlike vibration signal, which is regarded as the most famous metric in induction motor condition monitoring systems [2, 4].

However, thermal images are not commonly used in condition monitoring since defect data are limited or rare and are also subjected to a lack of fault diversity. It is common to use AI for classification or regression, and the neural network is expected to be trained on representative and balanced data for both. In fact, computers can also be used for data generation using generative models, such as variational autoencoders and generative adversarial networks. Therefore, the importance of using GANs arises when manufacturing needs a methodology that generates complex faults for better condition monitoring systems [1] it is difficult to obtain a sufficient defect data set in terms of diversity and quantity. A new generation method called surface defect-generation adversarial network (SDGAN. Generative Adversarial Networks (GANs) were introduced by Ian Goodfellow et al. in 2014 [5]. GANs use deep learning to generate fake images by mimicking the dataset distribution by playing a min-max game between two models, the Generator (G) and Discriminator (D) models. Hence, (G) learns to generate images very close to real images to fool D [6]. GANs are called generative because they generate something as an output, for example, images, videos domain adaptation, image super-resolution, etc., and adversarial because they have two networks fighting against each other (G) network (G) that capture the distribution and (D) model (D) that that tries to figure the genuinely of generated data if it was fake or real [7].

Deep Convolutional Generative Adversarial Network (DCGAN) is a type of GANs that Radford discovered, Metz, and Chintala in 2014 [8]. DCGAN utilises Convolutional Neural Network (CNN) architecture with GANs [1]it is difficult to obtain a sufficient defect data set in terms of diversity and quantity. A new generation method called surface defect-generation adversarial network (SDGAN. One of the key innovations of DCGAN is the replacement of pooling layers with stride convolutions and fractionally-strided convolutions. This allows both the (G) and (D) to learn convolutional operations, spatial downsampling, and upsample individually. By doing this, DCGAN ensures (G) and (D) networks learn independently, which can help to stabilise the training process. It also uses batch normalisation (BN) to stabilise learning. BN is a technique used to normalise the input to a layer, which helps to solve the vanishing gradient problem and prevent the deep (G) from collapsing all samples to the same points. Finally, DCGANs use both ReLU and LeakyReLU activation functions to allow the model to learn quickly and perform well [9], [10]computer graphics, and computer vision problems can be treated as image-to-image translation tasks. Such translation entails learning to map one visual representation of a given input to another representation. Image-to-image translation with generative adversarial networks (GANs. Followed by Data augmentation in fault diagnosis based on the Wasserstein Generative Adversarial Network with Gradient Penalty (WGAN-GP) deep architecture that can stabilise the training and generate high-quality images in 2017 [11]. WGAN-GP brings stability to the training model with almost no parameter tuning [12]. It also proved its capability in fault sample generation [13]a practical problem comes up in these studies, where deep learning models cannot be well trained and the classification accuracy is greatly affected because of the sample-imbalance problem, which means that there are a large amount of normal data but few fault samples. To solve the problem, an enhanced generative adversarial network (E-GAN, also in supplementing low dimensional fault data [14].

STATE-OF-THE-ART

DCGAN proved its efficiency in [15] which is called unbalanced dataset. Due to the existence of such unbalanced datasets, traditional methods are not easy to detect faults. Deep convolutional generative adversarial networks(DCGAN for image generation in solving imbalanced datasets in the chemical industry fault diagnosis field. It was also used in [4] for axial piston pump bearing fault diagnosis to mitigate data availability and missing fault labelling challenges. DCGAN was also used in induction motor fault classification using Case Western Reserve University's (CWRU) famous dataset in which CWT images were synthesised [14]. In January 2023, a paper was published focusing on WGAN usage in thermal images; fault creation in induction motors was also used to increase fault samples, namely, inner and outer faults also in healthy condition [16, 17]

It was clear from the literature that researchers tried to generate extra trustworthy data to enhance the training performance on limited fault types or generate look-like vibration signals without focusing on thermal image fault creation. Even the most recent paper explored generating thermal images on three conditions only to enhance the fault classification accuracy using a single input model. Unlike other projects, this paper explores the possibility of using GANs in induction motor thermal RGB image fault creation using DCGAN and WGAN. Hence, our condition monitoring thermal images are of high resolution and large size. The primary objective is to investigate the generation of an artificial thermal image dataset that resembles the existing dataset under various health conditions. The intention is to support the proposed multimodal condition-monitoring system outlined in the paper [2].

DATASET

Wolfson Magnetics Laboratory, located at Cardiff University School of Engineering. The laboratory conducted experiments to simulate six different failure modes and healthy conditions. To create these failure modes, a 2mm diameter drill was used to create holes in both the inner and outer parts of the bearing, as illustrated in Fig. 1 [3]. This paper aims to specifically investigate three conditions: inner, outer, which are (depicted in Fig. 1), and healthy. Healthy conditions refer to a bearing without any defects or faults.

However, Thermal images of bearing faults were collected using a Forward Looking InfraRed (FLIR) thermal camera

positioned 30cm from the centre of the housing, Fig. 2. The camera was connected to a computer to capture images of six artificially induced faults and one health condition. A total of 120 images were captured under three types of load, resulting in 360 images per condition. The data was split into 80% for training, equivalent to 288 RGB images, and 20% for testing, equal to 72 RGB photos [3, 18].

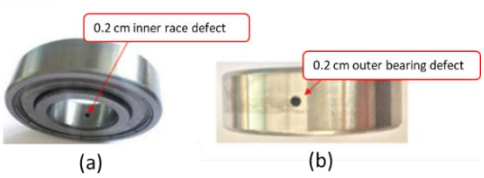

Fig. 1. Bearing faults (a) inner fault, (b) outer fault.

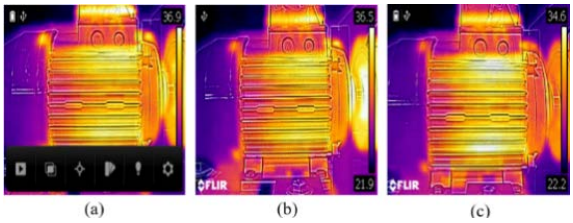

Fig. 2. Thermal images sample under three health conditions (a) inner fault (b) outer fault (c) healthy.

METHODOLOGY

In this study two GAN architectures were used. Firstly, the DCGAN model was trained on Google Colab using Tesla T4 GPU. Training and testing images of size 224 x 224 x 3 were located in the google drive directory. The (G) model takes a random noise vector of size 100 as input and generates an image. The (D) model predicts whether it is real or fake. Both models trained alternately with binary cross-entropy loss function and Adam optimiser. The DCGAN (G) has 40,635,715 parameters, and the (D) has 605,505 trainable parameters. The second architecture is WGAN-GP, a type of GAN architecture that uses a gradient penalty to enforce the Lipschitz continuity of the (D). The (D) is trained to output a scalar value instead of a probability. The (G) is trained to minimise the Wasserstein distance between the distribution of real and generated samples. The (G) loss is the negative Wasserstein distance, and the (D) loss is the difference between the average of the (D) output on the real samples and the generated samples, plus a gradient penalty term. The gradient penalty term is added to ensure that the (D) satisfies the Lipschitz continuity condition with a 0.0001 learning rate and batch size of 64 and Adam optimiser [11].

RESULTS

Basic DCGAN was tested on three health condition datasets: inner fault, outer fault, and healthy. The experiments varied in terms of hyperparameters, such as Learning Rate (LR) (0.0001, 0.0002), batch size (16,32), and the number of epochs (50, 500). On the other hand, WGAN-GP was tested on the inner fault type only with advanced training parameters, as shown in Table 1.

To evaluate the performance of each experiment, the (G) and (D) losses were assessed. A lower (D) loss relative to the (G) indicates superior (D) performance. Conversely, a lower (G) loss suggests a better performance of the (G). These findings align with the results presented in Table 1, where the performance of each model can be observed based on their respective losses. The experiments were conducted in two stages: the first stage involved using basic DCGAN with simple parameters (Experiments 1-12) to test various health condition datasets, while the second stage focused on utilising WGAN-GP with advanced parameters specifically for the inner fault type.

Stage 1: Three conditions were tested, starting with the inner fault (Experiments 1-4): longer training time led to better performance, with the best result observed in experiment 2. It used 500 epochs, LR of 0.0001, a batch size of 32, and achieved a (G) loss of 4.627 and a (D) loss of 0.0002. Outer fault (Experiments 5-8), Increasing the batch size led to better performance, with the best result obtained in experiment 7, which used 50 epochs, LR of 0.0002, a batch size of 16, and achieved a (G) loss of 0.0021 and (D) loss of

No.	Model	Dataset	LR	Batch Size	Epochs	Training time (min)	(G) Loss	(D) Loss
1	DCGAN	Inner	0.0001	16	500	48	3.2172	5.537
2	DCGAN	Inner	0.0001	32	500	41	4.627	0.0002
3	DCGAN	Inner	0.0002	16	50	5	0.0019	3.5658
4	DCGAN	Inner	0.0002	32	500	40	5.0668	7.6786
5	DCGAN	Outer	0.0001	16	50	4	0.0045	3.0554
6	DCGAN	Outer	0.0001	32	50	4	0.0079	2.782
7	DCGAN	Outer	0.0002	16	50	4	0.0021	3.4129
8	DCGAN	Outer	0.0002	32	50	4	0.00308	3.2324
9	DCGAN	Healthy	0.0001	16	50	4	0.00681	2.8419
10	DCGAN	Healthy	0.0001	32	50	4	0.0068	2.8419
11	DCGAN	Healthy	0.0002	16	50	5	0.00681	2.84186
12	DCGAN	Healthy	0.0002	32	500	50	8.32011	5.0697
13	WGAN-GP	Inner	0.0001	64	10,000	660 (11 hours)	-1896.8600	Loss Fake: -1897.3366 Loss Real: -1548.9419

Table 1. GAN performance for fault detection experiments.

3.4129. Healthy conditions (Experiments 9-12) where longer training time resulted in improved performance, with the best outcome observed in experiment 12, which utilised 1000 epochs, LR of 0.0002, a batch size of 32, and achieved a (G) loss of 8.3201 and a (D) loss of 5.0697. However, visual inspection results were not as promising compared to the project objective.

Stage 2: the inner fault was exclusively tested using WGAN-GP (Experiment 13) with a higher number of epochs and longer training time. The experiment required 11 hours of training time. The (G) loss was a high negative number, while the (D) loss of -1897.3366 for fake samples and -1548.9419 for real samples. These findings suggest that the (D) network performed well in distinguishing between real and fake samples, with the loss being minimised during training. Similarly, the (G) loss was also a high negative number, specifically -1896.8599. This indicates that the (G) successfully generates samples that the (D) classifies as real samples with a high level of confidence.

DISCUSSION

The choice of hyperparameters significantly impacts model performance. Generating artificial fault images of large size and high complexity posed challenges requiring significant time and GPU capabilities. Table 1 provides insights into the performance of GANs using DCGAN. Implementing WGAN-GP with advanced hyperparameters (10,000 epochs, batch size 64) on a GPU yielded efficient generation of motor images closely resembling real images over time as shown in Fig. 3.

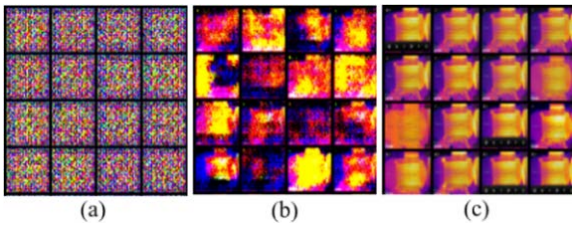

Fig. 3. WGAN-GP images (inner fault type): (a) at epoch 0, (b) at epoch 100, (c) at epoch 10,000.

CONCLUSION

This study has highlighted the significant impact of hyperparameters on GAN performance and has successfully demonstrated the remarkable capability of GANs in creating induction motor thermal images. This study has proved the applicability of WGAN-GP for generating artificial thermal images, although it requires high computational power. Future research will aim to optimise the process of dataset creation by training all fault types simultaneously using conditional GANs with higher image resolution.

Acknowledgements
This work was supported by the Saudi Arabian Cultural Bureau in London, the Saudi Arabian Ministry of Education, and Cardiff University.

Conflicts of interest
The authors declare no conflict of interest.

REFERENCES

[1] S. Niu, B. Li, X. Wang, and H. Lin, 'Defect Image Sample Generation With GAN for Improving Defect Recognition,' *IEEE Trans Autom Sci Eng*, vol. 17, no. 3, pp. 1–12, 2020. doi.org/10.1109/TASE.2020.2967415

[2] S. Hejazi, M. Packianather, and Y. Liu, 'Novel Preprocessing of Multimodal Condition Monitoring Data for Classifying Induction Motor Faults Using Deep Learning Methods,' in *2022 IEEE 2nd International Symposium on Sustainable Energy, Signal Processing and Cyber Security (iSSSC)*, Dec. 2022, pp. 1–6. doi.org/10.1109/iSSSC56467.2022.10051321

[3] F. McGhan, 'Transfer Learning for Induction Motor Fault Diagnosis,' 2020. https://github.com/frasermcghan/Year3Project (accessed Sep. 24, 2022).

[4] Y. He, H. Tang, Y. Ren, and A. Kumar, 'A semi-supervised fault diagnosis method for axial piston pump bearings based on DCGAN,' *Meas Sci Technol*, vol. 32, no. 12, p. 125104, Dec. 2021. doi.org/10.1088/1361-6501/ac1fbe

[5] I. Goodfellow *et al.*, 'Generative adversarial networks,' *Commun ACM*, vol. 63, no. 11, pp. 139–144, Oct. 2020, doi.org/10.1145/3422622

[6] A. Al-Qerem, Y. S. Alsalman, and K. Mansour, 'Image generation using different models of generative adversarial network,' *Proc - 2019 Int Arab Conf Inf Technol ACIT 2019*, pp. 241–245, 2019. doi.org/10.1109/ACIT47987.2019.8991120

[7] D. Saxena and J. Cao, 'Generative Adversarial Networks (GANs),' *ACM Comput Surv*, vol. 54, no. 3, 2021. doi.org/10.1145/3446374

[8] A. Kusiak, 'Convolutional and generative adversarial neural networks in manufacturing,' *Int J Prod Res*, vol. 58, no. 5, pp. 1594–1604, 2020. doi.org/10.1080/00207543.2019.1662133

[9] A. Alotaibi, 'Deep generative adversarial networks for image-to-image translation: A review,' *Symmetry* (Basel), vol. 12, no. 10, pp. 1–26, 2020. doi.org/10.3390/sym12101705

[10] Z. Wang, Q. She, and T. E. Ward, 'Generative Adversarial Networks in Computer Vision: A Survey and Taxonomy,' *ACM Comput. Surv.*, vol. 54, no. 2, 2021. doi.org/10.1145/3439723

[11] I. Gulrajani, F. Ahmed, M. Arjovsky, V. Dumoulin, and A. Courville, 'Improved Training of Wasserstein GANs,' Mar. 2017, [Online]. Available: http://arxiv.org/abs/1704.00028

[12] Z. Pan, W. Yu, X. Yi, A. Khan, F. Yuan, and Y. Zheng, 'Recent Progress on Generative Adversarial Networks (GANs): A Survey,' *IEEE Access*, vol. 7, pp. 36322–36333, 2019. doi.org/10.1109/ACCESS.2019.2905015

[13] R. Wang, S. Zhang, Z. Chen, and W. Li, 'Enhanced generative adversarial network for extremely imbalanced fault diagnosis of rotating machine,' *Meas J Int Meas Confed*, vol. 180, no. April, p. 109467, 2021. doi.org/10.1016/j.measurement.2021.109467

[14] H. Zhong, S. Yu, H. Trinh, Y. Lv, R. Yuan, and Y. Wang, 'Fine-tuning Transfer Learning based on DCGAN Integrated with Self-attention and Spectral Normalization for Bearing Fault Diagnosis,' *Measurement*, vol. 210, no. January, p. 112421, 2023. doi.org/10.1016/j.measurement.2022.112421

[15] Y. Du, W. Zhang, J. Wang, and H. Wu, 'DCGAN based data generation for process monitoring,' *Proc. 2019 IEEE 8th Data Driven Control Learn Syst Conf DDCLS 2019*, pp. 410–415, 2019. doi.org/10.1109/DDCLS.2019.890892

[16] H. Shao, W. Li, B. Cai, J. Wan, Y. Xiao, and S. Yan, 'Dual-Threshold Attention-Guided Gan and Limited Infrared Thermal Images for Rotating Machinery Fault Diagnosis Under Speed Fluctuation,' *IEEE Trans Ind Informatics*, pp. 1–10, 2023. doi.org/10.1109/TII.2022.3232766

[17] J. Ma, X. Jiang, B. Han, J. Wang, Z. Zhang, and H. Bao, 'Dynamic Simulation Model-Driven Fault Diagnosis Method for Bearing under Missing Fault-Type Samples', *Applied Sciences*, vol. 13, no. 5, p. 2857, Jan. 2023. doi.org/10.3390/app13052857

[18] A. K. Al-Musawi, F. Anayi, and M. Packianather, 'Three-phase induction motor fault detection based on thermal image segmentation,' *Infrared Phys Technol*, vol. 104, p. 103140, Jan. 2020. doi: 10.1016/j.infrared.2019.103140

Cynhadledd Ymchwil Peirianneg Caerdydd
Cardiff Engineering Research Conference

E. Spezi and M. Bray (eds.) 2024. *Proceedings of the Cardiff University Engineering Research Conference 2023.* Cardiff: Cardiff University Press.
doi.org/10.18573/conf1

Cardiff University Engineering Research Conference 2023 was organised by the School of Engineering and held from 12 to 14 July 2023 at Cardiff University.

The work presented in these proceedings has been peer reviewed and approved by the conference organisers and associated scientific committee to ensure high academic standards have been met.

Cardiff University Press | Gwasg Prifysgol Caerdydd

First published 2024

Cardiff University Press
Cardiff University, PO Box 430
1st Floor, 30-36 Newport Road
Cardiff CF24 0DE

cardiffuniversitypress.org

Editorial design and layout by
Academic Visual Communication

ISBN: 978-1-9116-5349-3 (PDF)